18. P. Fromherz, in *Electron Microscopy at Molecular Dimensions*, W. Baumeister and W. Vogell, Eds. (Springer-Verlag, Berlin, 1980), 338–349.
19. H. E. Ries and B. L. Meyers, *J. Appl. Polym. Sci.* **15**, 2023 (1971).
20. R. Aksberg and L. Ödberg, *Nord. Pulp Pap. Res. J.* **5**, 168 (1990).
21. Self-assembly deposition device (Riegler & Kirstein, Wiesbaden, Germany).
22. A. Laschewsky, *Eur. Chem. Chron.* **2**, 13 (1997).
23. Y. M. Lvov and G. Decher, *Crystallogr. Rep.* **39**, 628 (1994).
24. N. G. Hoogeveen, M. A. C. Stuart, G. Fleer, M. R. Böhmer, *Langmuir* **12**, 3675 (1996).
25. R. Advincula, E. Aust, W. Meyer, W. Knoll, *ibid.*, p. 3536.
26. D. Laurent and J. B. Schlenoff, *ibid.* **13**, 1552 (1997).
27. G. B. Sukhorukov, J. Schmitt, G. Decher, *Ber. Bunsenges. Phys. Chem.* **100**, 948 (1996).
28. J. J. Ramsden, Y. M. Lvov, G. Decher, *Thin Solid Films* **254**, 246 (1995).
29. R. G. Freeman *et al.*, *Science* **267**, 1629 (1995).
30. J. Schmitt *et al.*, *Adv. Mater.* **9**, 61 (1997).
31. S. W. Keller, H.-N. Kim, T. E. Mallouk, *J. Am. Chem. Soc.* **116**, 8817 (1994).
32. W. Kong *et al.*, *Makromol. Chem. Rapid Commun.* **15**, 405 (1994).
33. Y. Lvov, K. Ariga, T. Kunitake, *J. Am. Chem. Soc.* **117**, 6117 (1995).
34. E. R. Kleinfeld and G. S. Ferguson, *Science* **265**, 370 (1994).
35. G. S. Ferguson and E. R. Kleinfeld, *Adv. Mater.* **7**, 414 (1995).
36. E. R. Kleinfeld and G. S. Ferguson, *Chem. Mater.* **7**, 2327 (1995).
37. Y. Lvov, K. Ariga, I. Ichinose, T. Kunitake, *Langmuir* **12**, 3038 (1996).
38. Y. Lvov *et al.*, *ibid.* **10**, 4232 (1994).
39. D. L. Feldheim, K. C. Grabar, M. J. Natan, T. E. Mallouk, *J. Am. Chem. Soc.* **118**, 7640 (1996).
40. B. Philipp, H. Dautzenberg, K.-J. Linow, J. Kötz, W. Dawydoff, *Prog. Polym. Sci.* **14**, 91 (1989).
41. Z. Wang, T. Lan, T. J. Pinnavaia, *Chem. Mater.* **8**, 2200 (1996).
42. W. L. Ijdo, T. Lee, T. J. Pinnavaia, *Adv. Mater.* **8**, 79 (1996).
43. T. J. Pinnavaia, T. Lan, Z. Wang, H. Shi, P. D. Kaviratna, in *Nanotechnology: Molecularly Designed Materials*, vol. 622 of *ACS Symposium Series* (American Chemical Society, Washington, DC, 1996), pp. 250–261.
44. T. Lan and T. J. Pinnavaia, *Mater. Res. Soc. Symp. Proc.* **435**, 79 (1996).
45. R. Krishnamoorti, R. A. Vaia, E. P. Giannelis, *Chem. Mater.* **8**, 1728 (1996).
46. E. P. Giannelis, *Adv. Mater.* **8**, 29 (1996).
47. G. Decher and J. Schmitt, *Prog. Colloid Polym. Sci.* **89**, 160 (1992).
48. Y. Lvov, G. Decher, H. Möhwald, *Langmuir* **9**, 481 (1993).
49. H. Hong *et al.*, *Adv. Mater.* **7**, 846 (1995).
50. J. Schmitt *et al.*, *Macromolecules* **26**, 7058 (1993).
51. D. Korneev, Y. Lvov, G. Decher, J. Schmitt, S. Yaradaikin, *Physica B* **213–214**, 954 (1995).
52. G. Decher, Y. Lvov, J. Schmitt, *Thin Solid Films* **244**, 772 (1994).
53. H. Dautzenberg, J. Hartmann, S. Grunewald, F. Brand, *Ber. Bunsenges. Phys. Chem.* **100**, 1024 (1996).
54. W. Chen and T. J. McCarthy, *Macromolecules* **30**, 78 (1997).
55. M. Lösche, J. Schmitt, G. Decher, W. G. Bouwman, K. Kjær, in preparation.
56. F. Saremi, E. Maassen, B. Tieke, G. Jordan, W. Rammensee, *Langmuir* **11**, 1068 (1995).
57. G. J. Kellog *et al.*, *ibid.* **12**, 5109 (1996).
58. A. C. Fou and M. F. Rubner, *Macromolecules* **28**, 7115 (1995).
59. G. Decher, in *The Polymeric Materials Encyclopedia: Synthesis, Properties, and Applications*, J. C. Salamone, Ed. (CRC Press, Boca Raton, FL, 1996), vol. 6, 4540.
60. J.-D. Hong, K. Lowack, J. Schmitt, G. Decher, *Prog. Colloid Polym. Sci.* **93**, 98 (1993).
61. G. Decher, B. Lehr, K. Lowack, Y. Lvov, J. Schmitt, *Biosensors Bioelectronics* **9**, 677 (1994).
62. P.-G. He *et al.*, *Mater. Sci. Eng.* **C2**, 103 (1994).
63. P. T. Hammond and G. M. Whitesides, *Macromolecules* **28**, 7569 (1995).
64. T. G. Vargo *et al.*, *Supramol. Sci.* **2**, 169 (1996).
65. S. L. Clark, M. Montague, P. T. Hammond, *ibid.* **4**, 141 (1997).
66. W. B. Stockton and M. F. Rubner, *Macromolecules* **30**, 2717 (1997).
67. Y. Shimazaki, M. Mitsuishi, S. Ito, M. Yamamoto, *Langmuir* **13**, 1385 (1997).
68. G. Decher, *Nachr. Chem. Tech. Lab.* **41**, 793 (1993).
69. K. Chen, W. B. Caldwell, C. A. Mirkin, *J. Am. Chem. Soc.* **115**, 1193 (1993).
70. J. Schmitt, thesis, Johannes Gutenberg-Universität, Mainz, Germany (1996).
71. Y. Lvov, G. Decher, G. Sukhorukov, *Macromolecules* **26**, 5396 (1993).
72. G. B. Sukhorukov, H. Möhwald, G. Decher, Y. M. Lvov, *Thin Solid Films* **284–285**, 220 (1996).
73. Y. Lvov, K. Ariga, T. Kunitake, *Chem. Lett.* **1994**, 2323 (1994).
74. M. Gao *et al.*, *J. Chem. Soc. Chem. Commun.* **1994**, 2777 (1994).
75. N. A. Kotov, I. Dékány, J. H. Fendler, *J. Phys. Chem.* **99**, 13065 (1995).
76. ———, *Adv. Mater.* **8**, 637 (1996).
77. K. Ariga, Y. Lvov, M. Onda, I. Ichinose, T. Kunitake, *Chem. Lett.* **1997**, 125 (1997).
78. Y. Sun, X. Zhang, C. Sun, B. Wang, J. Shen, *Macromol. Chem. Phys.* **197**, 147 (1996).
79. M. Onda, Y. Lvov, K. Ariga, T. Kunitake, *Biotechnol. Bioeng.* **51**, 163 (1996).
80. ———, *J. Ferment. Bioeng.* **82**, 502 (1996).
81. R. von Klitzing and H. Möhwald, *Thin Solid Films* **284–285**, 352 (1996).
82. ———, *Macromolecules* **29**, 6901 (1996).
83. R. Pommersheim, J. Schrenzenmeir, W. Vogt, *Macromol. Chem. Phys.* **195**, 1557 (1994).
84. S. W. Keller, S. A. Johnson, E. S. Brigham, E. H. Yonemoto, T. E. Mallouk, *J. Am. Chem. Soc.* **117**, 12879 (1995).
85. X. Zhang, M. Gao, X. Kong, Y. Sun, J. Shen, *J. Chem. Soc. Chem. Commun.* **1994**, 1055 (1994).
86. T. M. Cooper, A. L. Campbell, R. L. Crane, *Langmuir* **11**, 2713 (1995).
87. A. Laschewsky *et al.*, *Thin Solid Films* **284–285**, 334 (1996).
88. J. K. Lee, D. S. Yoo, E. S. Handy, M. F. Rubner, *Appl. Phys. Lett.* **69**, 1686 (1996).
89. Y. Sun *et al.*, *J. Chem. Soc. Chem. Commun.* **1996**, 2379 (1996).
90. F. Saremi, G. Lange, B. Tieke, *Adv. Mater.* **8**, 923 (1996).
91. K. Ariga, Y. Lvov, T. Kunitake, *J. Am. Chem. Soc.* **119**, 2224 (1997).
92. P. Stroeve, V. Vasques, M. A. N. Coelho, J. F. Rabolt, *Thin Solid Films* **284–285**, 708 (1996).
93. M. Ferreira, M. F. Rubner, B. R. Hsieh, *Mater. Res. Soc. Symp. Proc.* **328**, 119 (1994).
94. J. Tian *et al.*, *Polym. Prepr. Am. Chem. Soc. Div. Polym. Chem.* **35**, 761 (1994).
95. A. C. Fou, O. Onitsuka, M. Ferreira, M. F. Rubner, B. R. Hsieh, *Mater. Res. Soc. Symp. Proc.* **369**, 575 (1995).
96. M. Onoda and K. Yoshino, *J. Appl. Phys.* **78**, 4456 (1995).
97. J. Tian *et al.*, *Adv. Mater.* **7**, 395 (1995).
98. J. Tian, C. C. Wu, M. E. Thompson, J. C. Sturm, R. A. Register, *Chem. Mater.* **7**, 2190 (1995).
99. A. C. Fou, O. Onitsuka, M. Ferreira, M. F. Rubner, B. R. Hsieh, *J. Appl. Phys.* **79**, 7501 (1996).
100. H. Hong *et al.*, *ibid.*, p. 3082.
101. B. Lehr, M. Seufert, G. Wenz, G. Decher, *Supramol. Sci.* **2**, 199 (1996).
102. O. Onitsuka, A. C. Fou, M. Ferreira, B. R. Hsieh, M. F. Rubner, *J. Appl. Phys.* **80**, 4067 (1996).
103. H. Hong *et al.*, *Supramol. Sci.* **4**, 67 (1997).
104. B. Lehr, J. Schmitt, R. Oeser, G. Decher, in preparation.
105. R. P. Feynman, in *Miniaturization*, H. D. Gilbert, Ed. (Reinhold, New York, 1961), pp. 282–296.

Computational Design of Hierarchically Structured Materials

G. B. Olson

A systems approach that integrates processing, structure, property, and performance relations has been used in the conceptual design of multilevel-structured materials. For high-performance alloy steels, numerical implementation of materials science principles provides a hierarchy of computational models defining subsystem design parameters that are integrated, through computational thermodynamics, in the comprehensive design of materials as interactive systems. Designed properties combine strength, toughness, and resistance to impurity embrittlement. The methods have also been applied to nonferrous metals, ceramics, and polymers.

For millennia, materials have been developed through the empirical correlation of processing and properties. The past century has seen the formation of a science of materials that has defined the structural basis of materials behavior, but its role has primarily been to explain the products of empiricism after their development. In the past decade, the numerical implementation of materials science principles and the integration of resulting computational capabilities within a systems engineering framework has given birth to a revolutionary approach (*1*) in the form of quantitative conceptual design of materials.

The author is in the Department of Materials Science and Engineering, Northwestern University, 2225 North Campus Drive, Evanston, IL 60208–3108, USA.

Materials as Systems

This approach to materials design is based on the philosophy of the late Cyril Stanley Smith (*2*, *3*). Smith wrote extensively about interactive structural hierarchy in materials (and space-filling aggregates in all branches of science, including geology and biology). He envisioned a multilevel structure with strong interactions among levels, with an inevitable interplay of perfection and imperfection, and a duality of description in which structure can be equivalently regarded in terms of space-filling units or of the array of interfaces that bound them. This view of materials admits a necessary complexity.

In the modern form of materials science, Zener (*4*) has added a recognition of the dynamic nature of materials to Smith's spatial hierarchy. In association with a hierarchy of length scales, there is a spectrum of characteristic relaxation times (and therefore a spatiotemporal hierarchy), so that in any real structure, there is some level (such as the interatomic level or the grain boundary level) that has not had time to equilibrate. Thus, real structures are nonequilibrium and are therefore path- (or history-) dependent, and recognizing this intrinsic dynamic nature further raises the essential complexity of materials.

Complexity sets natural limits on the degree of predictability. It is often argued that the complexity of materials makes them undesignable. But this would be so only if design required total predictability. Fortunately, another principle can be applied, one that Cohen (*5*) has termed "reciprocity," which can be illustrated by the example of structure-property relations. Although properties are typically regarded as being controlled by structure, Cohen argues that structure can be equally regarded as being controlled by properties, in that the perception of structure is governed by the properties that need to be understood. If a complex structure is examined from the viewpoint of specific properties, useful relations can be established. Much of materials science is the art of discriminating the essential from the nonessential (the latter being similar to the evolutionary vestiges of the biological world) as the products of empirical development are unraveled to control desired properties. Reciprocity then allows scientific analysis to provide the tools for materials design.

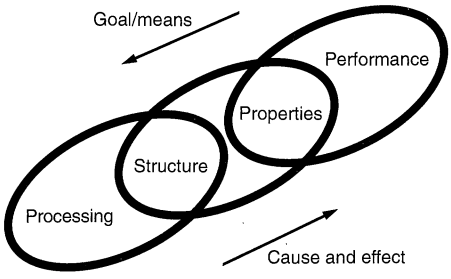

Fig. 1. Three-link chain model of the central paradigm of materials science and engineering.

Although the powerful simplifying methods of scientific analysis provide the raw ingredients for design, these methods do not integrate results so that new complexity can be created and controlled. For this purpose, engineering has developed the systems approach. A concise summary of the approach, which is used in a materials design course at Northwestern University (*6*), is given in a review paper by Jenkins (*7*) of the Open University. System analysis begins with problem identification, organization of an appropriate interdisciplinary team, formulation of system design objectives from the function of the system in the wider system it serves (adopting a user-centered perspective), and identification of component subsystems and their interactions, typically represented in a flow-block diagram. Design synthesis starts with development and validation of appropriate (purposeful) models for subsystems and their interactions, assigning priorities and needed accuracy from the context of the design problem, followed by model integration to generate candidate design solutions offering satisfactory compromise among conflicting objectives. The implementation of prototypes then allows their experimental evaluation at the level of the models that created them, providing feedback for iterative reanalysis and design until objectives are met. Specifications can then be set for operation of the designed system.

In the context of materials, the prevalent practice of empirical development involves minimal up-front theoretical analysis and a large amount of parallel (and relatively superficial) evaluation of prototypes that leads to empirical correlations that produce materials with limited predictability of behavior. In an age of increasing cost of experiment and decreasing cost (and increasing power) of computation-based theory, a design approach making maximum use of science-based mechanistic models and the sequential, deeper evaluation of a small number of prototypes can not only reduce the time and cost of initial development but produce designed materials with more predictable behavior. This approach can also reduce the time and cost of process scale-up and material qualification.

Founded in 1985 with initial National Science Foundation (NSF) support, the Steel Research Group (SRG) (*1*), an international effort that includes several labs from industry, academia, and government, has adapted such a systems methodology to the science-based design of materials for the production of high-performance alloy steels. The research has integrated physical and process metallurgy, ceramics, applied mechanics, quantum physics, chemistry, mechanical engineering, and management science. Projects have investigated ultrahigh-strength martensitic alloy steels, high-strength formable automotive sheet steels, and ferritic superalloys for power-generating turbine applications. The examples discussed here are drawn primarily from the largest project on martensitic alloy steels, which has more recently led to a project focused on high-performance gear and bearing steels. This class of steels undergoes a diffusionless (martensitic) structural transformation during quenching from high temperatures, to provide a fine microstructure offering the best combination of strength and toughness.

The materials property objectives motivating the research were developed with a property cross-plot approach, as generalized by Ashby (*8*) to quantify property-performance relations in a broad methodology for materials selection. The exercise defined combinations of strength (resistance to permanent deformation), toughness (fracture resistance), and resistance to environmental hydrogen (H) cracking that would allow a major advance in the useable strength level of structural steels, an advance that was recognized by industry participants as being beyond the reach of empirical development in the planned time frame.

Four primary elements are critical in materials science and engineering: processing, structure, properties, and performance (*9*). There is no general agreement, however, on how these elements are interconnected. SRG research has found the linear structure shown in Fig. 1 to be crucial for systematic design. In the spirit of Smith's structural duality, Fig. 1 emphasizes that these elements form a three-link chain. Expanding Cohen's reciprocity, the structure offers a resonant bond between the science and engineering of materials, in which the deductive cause-and-effect logic of science flows to the right, while the inductive goal-means relations of engineering flow to the left. Further support for the utility of this paradigm is offered by its direct correspondence to the general axiomatic design approach developed by Suh and Albano (*10*) to apply across all engineering disciplines.

Once a set of property objectives has been deduced from property-performance relations, the chain of Fig. 1 can serve as a backbone to which the addition of Smith's hierarchy can provide a first-order representation of a full system structure. The product of such an exercise as applied to the system structure of a high-performance alloy steel in SRG research (*1*) is represented in Fig. 2. The chart denotes the microstruc-

tural subsystems controlling the properties of interest, and the substages of processing (represented by a vertical process flow chart) governing the evolution of each subsystem. This representation of the full system was used to identify and prioritize the key structure-property and process-structure links to be quantified by the basic research of the SRG program.

Computational design of hierarchical structure requires a hierarchy of design models. Fig. 3 represents the computational models developed from research on the primary microstructural levels of Fig. 2. The experimental techniques used to create and validate these models are shown on the left; acronyms summarized on the right denote specific models and their software platforms.

The primary design tool used in this research for integrating the output of subsystem models was the THERMOCALC (TC) thermochemical database and software system (*11*) developed at the Royal Institute of Technology in Stockholm. Specifying subsystem requirements in terms of thermodynamic parameters, the flexible TC system is used to solve for complete alloy compositions that are capable of achieving desired microstructures under prescribed processing conditions. Recognizing the dynamic nonequilibrium nature of real microstructures, it should be emphasized that the thermodynamic parameters of interest rarely concern equilibrium states, but rather specify length scales and time scales of evolving metastable (or unstable) states. A remarkable degree of control of dynamic systems can be achieved through control of the thermodynamic forces that drive them.

Subsystem Modeling

The development of science-based computational subsystem models through focused basic research is reviewed briefly below.

Strength subsystems. As denoted at the highest structural levels in Figs. 2 and 3, a primary consideration in strengthening is control of the structural transformation during quench hardening of an ultrahigh-strength steel. The desired class of microstructure (denoted "lath martensite" in Fig. 2 and depicted at the top of Fig. 3) requires a diffusionless martensitic structural transformation at 200°C or above. After refining the TC thermodynamic database, the development of a kinetic parameter database based on current transformation theory (*14*) provided the required computational model (MART) to predict transformation temperatures with required precision. Model predictions are validated by metallurgical quenching dilatometry (MQD), differential scanning calorimetry (DSC), light microscopy (LM), and transmission electron microscopy (TEM). Other transformation design codes shown in Fig. 3 (CASSIS and MAP) treat the kinetic competition with other structural transformations in the case of lower alloy steels.

The second structural level shown in Fig. 2 represents the final stage of strengthening by solid-state precipitation of alloy carbides during the last stage of heat treatment (*13*). The precipitation of ultrafine carbides corresponds to the "nano design" level in Fig. 3, represented by a model computation of the chemical composition field in the Fe-base matrix surrounding an ellipsoidal nanometer-scale carbide particle (*14*). At such small length scales, suppression of conventional structural relaxation processes promotes the continuity of crystal planes across the particle-matrix interface, causing extreme elastic distortion, and interfacial energy makes a dominant contribution to the thermodynamics governing particle size. Measurements of particle size by small-angle neutron scattering (*15*) (SANS), elastic distortion by x-ray diffraction (XRD), particle composition by atom-probe field-ion microscopy (*16*) (APFIM) and analytical electron microscopy (AEM), and calculations of elastic energies from continuum mechanics methods (*14*) (ABAQUS/EFG) are integrated with the TC thermodynamics [TC (Coh)]

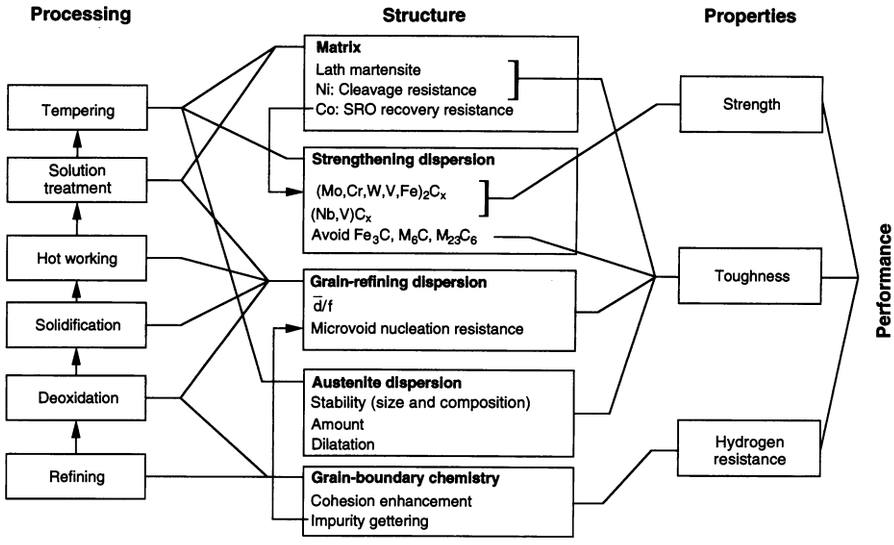

Fig. 2. Materials system chart for high-performance alloy steel (*1*).

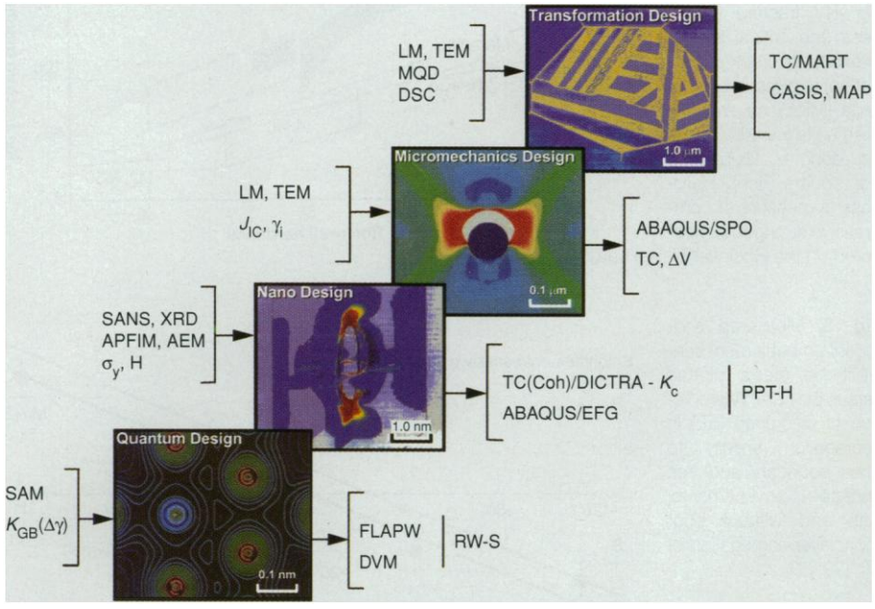

Fig. 3. Hierarchy of computational design models and the experimental tools used to create and validate them. Abbreviations are defined in the text.

to deduce interfacial energies. Precipitation rate constants (K_c) are predicted (*17*) by use of the DICTRA diffusion software and database. These results are combined to generate a comprehensive model (PPT-H) for the evolution of alloy strength σ_y (controlled by particle size and spacing) during precipitation hardening. The resulting accuracy of particle size control has allowed the design of alloy compositions with efficient strengthening dispersions, achieving 50% greater strength at a given alloy carbon content.

Toughness subsystems. A primary concern in fracture resistance is maintenance of a sufficiently fine polycrystalline grain size in order to inhibit competing brittle fracture mechanisms that allow fracture with less energy absorption. The grain size established during high-temperature heat treatments is determined by the geometry of a stable "grain-refining" particle dispersion, denoted by the third structural level of Fig. 2, which impedes the high-temperature grain boundary motion that is responsible for normal grain coarsening. Once sufficient grain refinement is achieved to promote fracture by higher toughness ductile-fracture processes, the actual level of fracture toughness becomes limited by the formation of microvoids, which occurs through interfacial separation at the grain-refining particles themselves (*18*). Simulation of such processes uses traditional continuum mechanics methods, as denoted by the micromechanics design level in Fig. 3. Such simulations (*19*, *20*) have demonstrated the mechanism by which microvoids drive ductile fracture and have quantified the role of dispersion geometry (including average particle size $\bar{d}$ and volume fraction f) and particle interfacial properties as the basis for thermodynamic component selection and processing optimization in materials design (*21*). Experimental validation of models employs measurements of fracture energy absorption (J_{IC}) and critical plastic strain for strain localization (γ_i) in shear tests.

As denoted by the fourth structural level of Fig. 2, further resistance to microvoid fracture can be obtained through mechanical interaction with a fine dispersion of transformable particles (precipitated during final heat treatment), which can undergo a strain-induced structural transformation during ductile fracture (*22*). Using a matrix flow model (ABAQUS/SPO) (*23*) based on the kinetics of such transformations, the micromechanics simulation in Fig. 3 represents the computed contours of the fraction of the transformed phase produced during microvoid formation in such a material (*24*). The simulations demonstrate the role of pressure-sensitive transformation kinetics in stabilizing plastic flow during microvoid growth, and they define guidelines for optimizing transformation thermodynamic stability and dilatancy (ΔV). Based on TC thermodynamic modeling incorporating these guidelines, the dark bands denoted "TT" in Fig. 4 depict the toughness-hardness combinations achieved through multistep heat treatments controlling microstructure to exploit such transformation toughening. Properties achieved in the new commercial AerMet100 and an experimental alloy designated MTL1 (*25*) lie within the original SRG objectives box denoted by the dashed lines.

Embrittlement resistance subsystems. Denoted by the last structural level in Fig. 2, environmental cracking of ultrahigh-strength steels occurs by an intergranular mechanism associated with the combined effects of environmental H and the prior segregation of embrittling impurities (*26*). Understanding its underlying mechanism has required the most fundamental and interdisciplinary research of the SRG effort, combining applied mechanics, materials science, and quantum physics.

A crucial contribution has come from the work of Rice and Wang (*27*) in modeling the mechanics and thermodynamics of interfacial separation. A key prediction is that the embrittlement potency of a segregating solute should scale with the difference in its energies of segregation to the free surface (FS) versus a grain boundary (GB). Reported data for embrittlement potency in steels, measured as the shift in ductile-brittle transition temperature per amount of segregant [K/atomic%, with atomic% measured by scanning auger microanalysis (SAM)], shows a compelling correlation with this segregation energy difference, based on available thermodynamic data (*27*).

Based on this thermodynamic description of intergranular embrittlement, a series of electronic-level total energy calculations has used both the full-potential linear augmented plane wave (FLAPW) method (*28*) and the cluster discrete variation method (DVM), as represented by the valence charge-density contour plot denoted "quantum design" in Fig. 3. Although materials science has contributed the basic atomic structural models to support such calculations, a pivotal development has been the ability to compute interatomic forces within the FLAPW code to allow precise detailed atomic relaxations within the same method. The latest results (*29*, *30*) are summarized in Fig. 5, which plots the experimental embrittlement potencies against the quantum mechanical theoretical predictions of the segregation energy difference ΔE, with and without the prior segregation of a monolayer of Mn, representing the most common alloying element in steels. The theoretical thermodynamics show a stronger correlation with embrittlement than the available experimental thermodynamics, particularly when Mn is taken into account. Cor-

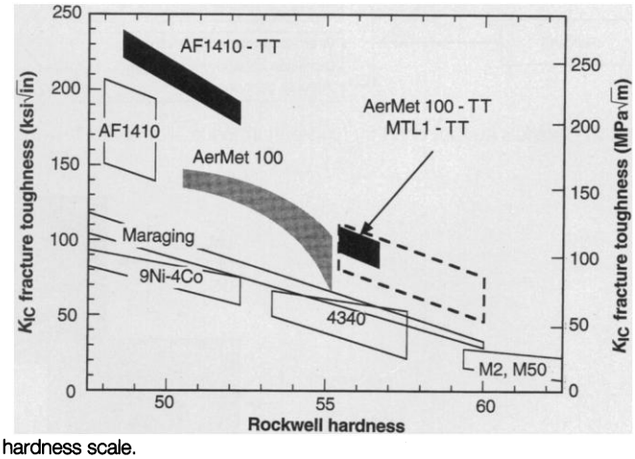

Fig. 4. Toughness-hardness plot of various steels. Dark bands for steels with TT designation show property improvement through multistep tempering to provide transformation toughening. K_{IC} fracture toughness (the critical stress-intensity for crack propagation) is given in both SI units (MPa$\sqrt{m}$) and English units (ksi$\sqrt{in}$, where ksi denotes kilopounds per square inch). Hardness (a measure of compressive strength) is measured on the Rockwell C (R_c) hardness scale.

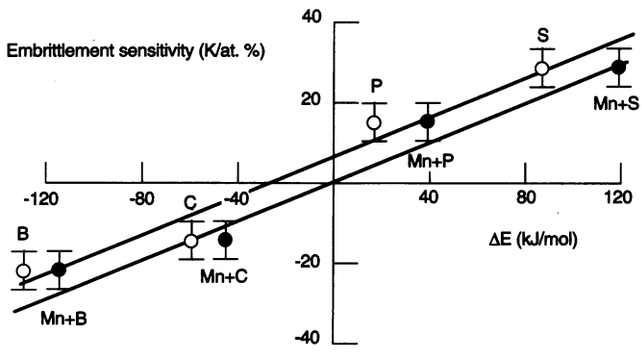

Fig. 5. Measured segregant embrittlement sensitivity in steels plotted versus the FLAPW prediction of difference (ΔE) in segregation energy to grain boundary and free surface environments, with and without prior monolayer segregation of Mn (*29*, *30*).

relation of measured grain boundary (GB) toughness (K_{GB}) with the ideal work of interfacial separation ($\Delta\gamma$) based on the FLAPW predictions has provided a modified Rice-Wang model (RW-S) for the design of grain boundary cohesion.

More important than the ability to determine these key energy differences is the ability to establish their underlying electronic basis. Computed charge-transfer plots, together with density-of-states curves and detailed electronic orbital plots, demonstrate that embrittling P and S undergo a nonhybridized electrostatic interaction with Fe, which is more adaptive to the FS environment, whereas the cohesion-enhancing B and C exhibit anisotropic hybridized bonding across the GB. Such calculations further reveal that the embrittling effect of Mn is associated with promotion of in-plane bonding, which preferentially stabilizes the FS.

The most recent improvements in precision have now made possible a definitive calculation of the effect of H on Fe GB cohesion (*31*). In contrast to the hybridized versus electrostatic interactions displayed by the segregants shown in Fig. 5, H shows a third class of behavior that is more ionic in character. The underlying energetics of H embrittlement are associated with enhanced charge transfer from Fe to H in the FS environment. The intrinsic embrittlement potency per atom is comparable to that of P, which is consistent with experimental estimates (*32*), whereas it is well established that its effective potency is greatly amplified by its mobility (*32*). The small magnitude of this intrinsic potency, and the determination of its origin in charge transfer, offer the hope for its reversal or cancellation by predictive alloying.

The insights provided by these new predictive capabilities promise a new generation of "quantum steels" in which, analogous to semiconductors, boundaries are deliberately doped to attain desired electronic structures for enhanced intrinsic cohesion and altered interaction with impurities, including H.

Although the electronic-level approach offers the greatest potential for improvements, significant advances in environmental cracking resistance have already been demonstrated under SRG research through thermodynamics-based design of novel impurity-gettering phases such as lanthanum phosphate ($LaPO_4$), which, when accessed by appropriate processing, remove embrittling impurities from the grain boundaries (*33*, *34*).

Design Examples

An effort to integrate these developing principles into the comprehensive design of a new alloy was undertaken by a team of students in the first materials design class at Northwestern University in 1989. The problem adopted was the design of a secondary-hardening stainless steel for use in bearings in the fuel and oxidizer turbopumps of the space shuttle main engine (SSME). The property objectives obtained from NASA and Rocketdyne engineers were Rockwell hardness R_c60 for wear and contact fatigue resistance, with a doubling of toughness and H resistance as compared with the current 440C alloy. Adopting the system structure of Fig. 2, composition was constrained for $LaPO_4$ impurity gettering for enhanced H resistance, while the matrix was constrained to contain a minimum of 12 weight % Cr for corrosion resistance. Estimating 0.30 weight % C as sufficient to maintain R_c60, based on the strengthening models, a line of Ni and Co compositions was computed to maintain a sufficiently high transformation temperature to yield a martensitic structure. Along this line, the computed thermodynamic stability and amount of transformation-toughening particles provided a unique Ni and Co content. With these composition variables fixed, Mo and V concentrations were optimized for the thermodynamics of precipitation strengthening, constrained by solubility limits at solution treatment temperatures. Under a grant from NASA, a prototype alloy was evaluated, and it demonstrated the desired doubling of fracture toughness at the required hardness level (*35*).

A related area of long-term interest has been the design of a new class of alloy steels for case-hardening gear and bearing applications. Research in this area was initiated with a property-performance analysis by a team of senior project students in mechanical engineering, who identified property objectives to allow a 50% reduction in gear weight. A team of students in materials design class then performed conceptual designs aimed at achieving these objectives by using recent strengthening models. Figure 6 depicts the increased hardness profile so far obtained in prototype gear steels (*36*). The fatigue properties are currently under evaluation, with promising preliminary results. A related custom gear steel is undergoing gear testing by the Newman-Haas Indycar racing team.

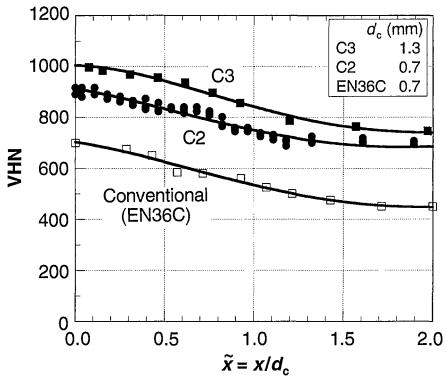

Fig. 6. Hardness profile for carburized prototype gear steels (C3 and C2) compared with conventional (EN36C) gear steel (*36*). Hardness is measured on the Vickers (VHN) scale. Distance x is normalized to the effective case depth d_c.

The range of design projects considered by the most recent materials design class is wide-ranging and includes not only alloy steel projects derived from SRG research but also nonferrous projects that test the generality of the design methodology and also explore the level of conceptual design that can be practiced without support from a major research project. This has included projects in ceramics and polymers. The ceramic project has assessed the feasibility of achieving processing and property requirements for dental fillings using Portland cement–based hydrate ceramic composites as a cost-effective replacement for mercury amalgams, and has so far included TC representation of metastable phase relations in the hydration of calcium silicates. The polymer project has explored the transfer of the gradient system technology of steel gears to case-hardening of plastics. Rubber-toughened epoxy systems have been identified as being most promising for achieving hardness gradients, controlled residual stress, and core toughness. The TC modeling of phase separation behavior during curing has aided process models for achieving desired phase fraction gradients.

The most ambitious design project has been the "Terminator 3" self-healing, biomimetic, smart steel composite. A number of biomimetic concepts have been combined, starting with natural seashell, tooth, and bone architectures. These structures typically involve the reinforcement of a brittle ceramic by a rubbery polymeric component to provide "crack bridge" toughening in which rubbery ligaments stretch across cracks. More sophisticated adaptive behavior is exhibited by viruses and bacteria, which exploit martensitic structural transformations in cylindrical protein crystals to use reversible strain phenomena such as superelasticity and shape-memory effects (*37*).

A system integrating these concepts in an all-metallic composite consists of a precipitation-strengthened high-temperature superalloy reinforced by a thermodynamically compatible, precipitation-strengthened, shape memory alloy. The low-temperature brittleness of the superalloy is compensated for by crack bridging through martensitic transformation superelasticity that is analogous to the rubbery polymer reinforcement of the seashell system. After bridging of low-temperature damage, when the superalloy is returned to its operating temperature, the bridging ligaments contract by means of the shape memory effect to clamp the cracks closed. If the memory alloy has sufficiently greater strength, the clamping force can be maintained to promote

diffusional rewelding of the damage, thus providing the ultimate biomimetic property of self healing.

Thermodynamic compatibility of the pair of two-phase alloys requires a four-phase equilibrium at operating temperatures and a two-phase equilibrium during solution treatment. A preliminary thermodynamic feasibility analysis, including assessment of memory alloy stability requirements, was performed by a team of juniors in materials design class. Continued evaluation (*38*) has included a test of mechanical concepts that uses a TiNi-reinforced Sn alloy composite prototype to demonstrate both macroscopic strain reversal and the desired crack-clamping behavior (*41*). Precise multicomponent phase relations for the Fe-based system have been evaluated with diffusion couple experiments, and prototype steel composites are being fabricated.

The success of these initial designs suggests that the integration of computational materials science within a systems engineering framework offers a powerful new approach for the creation of superior materials that have sophisticated control of a multilevel dynamic structure, combined with reduced time and cost of materials development. These first steps herald a new synergy of the science and engineering of materials.

REFERENCES AND NOTES

1. G. B. Olson, M. Azrin, E. S. Wright, Eds., *Innovations in Ultrahigh-Strength Steel Technology* [Government Printing Office (GPO), Washington, DC, 1990].
2. C. S. Smith, *A Search for Structure* (MIT Press, Cambridge, MA, 1981).
3. _____, in *Martensite*, G. B. Olson and W. S. Owen, Eds. (ASM International, Materials Park, OH, 1992), pp. 21–39.
4. C. Zener, *Elasticity and Anelasticity of Metals* (Univ. of Chicago Press, Chicago, IL, 1948).
5. M. Cohen, *Mat. Sci. Eng.* **25**, 3 (1976).
6. G. B. Olson, in *M. E. Fine Symposium*, P. K. Liaw, J. R. Weertman, H. L. Markus, J. S. Santner, Eds. (The Minerals, Metals & Materials Society (TMS) of the American Institute of Mining, Metallurgical, and Petroleum Engineers (AIME), Warrendale, PA, 1991), p. 41.
7. G. M. Jenkins, in *Systems Behaviour*, J. Beishon and G. Peters, Eds. (Harper and Row, London, for Open Univ. Press, 1972), pp. 56–82.
8. M. F. Ashby, *Materials Selection in Mechanical Design* (Pergamon, Tarrytown, NY, 1992).
9. COSMAT Summary Report, *Materials and Man's Needs* (National Academy of Sciences, National Academy Press, Washington, DC, 1974); *Materials Science and Engineering for the 1990s* (National Research Council, National Academy Press, Washington, DC, 1989).
10. N. P. Suh, *The Principles of Design* (Oxford Univ. Press, New York, 1990); L. D. Albano and N. P. Suh, *Res. Eng. Des.* **4**, 171 (1992).
11. B. Sundman, B. Jansson, J. O. Andersson, *CALPHAD* **9**, 153 (1985).
12. G. Ghosh and G. B. Olson, *Acta Metall. Mater.* **42**, 3361 (1994).
13. G. R. Speich, in *Innovations in Ultrahigh-Strength Steel Technology*, G. B. Olson, M. Azrin, E. S. Wright, Eds. (GPO, Washington, DC, 1990), pp. 89–111.
14. K. C. King, P. W. Voorhees, G. B. Olson, *Metall. Trans.* **22A**, 2199 (1991).
15. A. J. Allen, D. Gavillet, J. R. Weertman, *Acta Metall.* **41**, 1869 (1993).
16. G. B. Olson, T. J. Kinkus, J. S. Montgomery, *Surf. Sci.* **246**, 238 (1991).
17. A. Umantsev and G. B. Olson, *Scr. Metall.* **29**, 1135 (1993).
18. J. G. Cowie, M. Azrin, G. B. Olson, *Metall. Trans. A* **2A**, 143 (1989).
19. A. Needleman, in *Innovations in Ultrahigh-Strength Steel Technology*, G. B. Olson, M. Azrin, E. S. Wright, Eds. (GPO, Washington, DC, 1990), pp. 331–346.
20. Y. Huang and J. W. Hutchinson, in *Modelling of Material Behavior & Design*, J. D. Embury, Ed. (TMS-AIME, Warrendale, PA, 1990), pp. 129–148.
21. M. J. Gore, G. B. Olson, M. Cohen, in *Innovations in Ultrahigh-Strength Steel Technology*, G. B. Olson, M. Azrin, E. S. Wright, Eds. (GPO, Washington, DC, 1990), pp. 425–441.
22. G. B. Olson, *J. Phys. V*, Colloque C1, 407 (1996).
23. R. G. Stringfellow, D. M. Parks, G. B. Olson, *Acta Metall.* **40**, 1703 (1992).
24. S. Socrate, thesis, Massachusetts Institute of Technology (1996).
25. C. J. Kuehmann, J. Cho, T. A. Stephenson, G. B. Olson, in *Metallic Materials for Lightweight Applications*, E. B. Kula and M. G. H. Wells, Eds. (GPO, Washington, DC, 1994), pp. 337–355.
26. C. J. McMahon Jr., in *Innovations in Ultrahigh-Strength Steel Technology*, G. B. Olson, M. Azrin, E. S. Wright, Eds. (GPO, Washington, DC, 1990), pp. 597–618.
27. J. R. Rice and J.-S. Wang, *Mater. Sci. Eng. A* **107**, 23 (1989).
28. R. Wu, A. J. Freeman, G. B. Olson, *Science* **265**, 376 (1994).
29. _____, *Phys. Rev. B* **53**, 7504 (1996).
30. L. Zhong, R. Wu, A. J. Freeman, G. B. Olson, *ibid.* **55**, 11 135 (1997).
31. _____, unpublished results
32. P. M. Anderson, J. S. Wang, J. R. Rice, in *Innovations in Ultrahigh-Strength Steel Technology*, G. B. Olson, M. Azrin, E. S. Wright, Eds. (GPO, Washington, DC, 1990), pp. 619–649.
33. J. F. Watton, G. B. Olson, M. Cohen, in *Innovations in Ultrahigh-Strength Steel Technology*, G. B. Olson, M. Azrin, E. S. Wright, Eds. (GPO, Washington, DC, 1990), pp. 705–737.
34. G. Ghosh and G. B. Olson, in *Proceedings of 51st Annual Meeting of the Microscopy Society of America*, G. W. Bailey and C. L Rieder, Eds. (San Francisco Press, San Francisco, CA, 1993).
35. T. A. Stephenson, C. E. Campbell, G. B. Olson, *Advanced Earth-to-Orbit Propulsion Technology 1992*, R. J. Richmond and S. T. Wu, Eds., *NASA Conf. Publ. 3174* (1992), vol. 2, pp. 299–307.
36. J. Wise, unpublished results.
37. G. B. Olson and H. Hartman, *J. Physique* **43**, C4–855 (1982).
38. B. Files, thesis, Northwestern University (1997).
39. G. B. Olson, K. C. Hsieh, H. K. D. H. Bhadeshia, in *Microstructures LCS '94* (Iron and Steel Institute of Japan, Tokyo, 1994).

40. The Northwestern component of the SRG program has been sponsored by the Office of Naval Research, the Army Research Office, NSF, NASA, the U.S. Department of Energy, the Electric Power Research Institute, and the Air Force Office of Scientific Research, with industry gifts and fellowship support.

Molecular Manipulation of Microstructures: Biomaterials, Ceramics, and Semiconductors

Samuel I. Stupp* and Paul V. Braun

Organic molecules can alter inorganic microstructures, offering a very powerful tool for the design of novel materials. In biological systems, this tool is often used to create microstructures in which the organic manipulators are a minority component. Three groups of materials—biomaterials, ceramics, and semiconductors—have been selected to illustrate this concept as used by nature and by synthetic laboratories exploring its potential in materials technology. In some of nature's biomaterials, macromolecules such as proteins, glycoproteins, and polysaccharides are used to control nucleation and growth of mineral phases and thus manipulate microstructure and physical properties. This concept has been used synthetically to generate apatite-based materials that can function as artificial bone in humans. Synthetic polymers and surfactants can also drastically change the morphology of ceramic particles, impart new functional properties, and provide new processing methods for the formation of useful objects. Interesting opportunities also exist in creating semiconducting materials in which molecular manipulators connect quantum dots or template cavities, which change their electronic properties and functionality.

The functionality of materials in macroscopic form is seldom achieved with pure chemical compounds that form single crystals. Many of nature's remarkable materials contain mixtures of molecules or microstructures in which inorganic crystals or glasses coexist with organic molecules. Examples include bone, cartilage, shells, leaves, and skin. Here, we address the concept of molecular manipulation of microstructures in inorganic materials, a biologically inspired synthetic tool for the era of

The authors are in the Department of Materials Science and Engineering, Department of Chemistry, Beckman Institute for Advanced Science and Technology, Materials Research Laboratory, University of Illinois at Urbana-Champaign, Urbana, IL 61801, USA.

*To whom correspondence should be addressed.